Design and synthesis of symmetrical pentamethine cyanine dyes as NIR photosensitizers for PDT

Betty Ciubini[a], Sonja Visentin[b], Loredana Serpe[c], Roberto Canaparo[c], Andrea Fin[d] and Nadia Barbero[a,*]

[a]Department of Chemistry and NIS Interdepartmental Centre, University of Torino, via Pietro Giuria 7, 10125 Torino, Italy.
[b]Molecular Biotechnology and Health Sciences Department, University of Torino, via Quarello 15, 10135 Torino, Italy.
[c]Department of Drug Science and Technology, University of Torino, via Pietro Giuria 13, 10125 Torino, Italy.
[d]Department of Chemistry and Biochemistry, University of California, San Diego, La Jolla, California 92093-0358, United States Corresponding author. E-mail address: nadia.barbero@unito.it (N. Barbero).

Keywords

Cyanine dyes, Near Infra-Red (NIR), photosensitizers, photodynamic therapy (PDT).

Abstract

Herein, we report the synthesis and spectroscopic characterization of novel Near Infra-Red (NIR) pentamethine cyanine dyes, as potential photosensitizers for Photodynamic Therapy (PDT) characterized by a strong absorption in the tissue transparency window (600-800 nm). The heteroaromatic benzoindolenine ring of various symmetrical cyanine dyes has been differently functionalized and quaternarized as a result of a structure-activity study and to determine the substituent effect on the cellular uptake, ROS production and photodynamic activity. These probes present low cytotoxicity in dark, but promote phototoxic effect, upon irradiation, in human fibrosarcoma cell line (HT-1080) with interesting and unexpected structure to property activity.

1. Introduction

NIR dyes had a significant development in bioanalytical or biologically related applications in recent years with a particular focus on *in vivo* fluorescence imaging due to the low self-fluorescence of the biological molecules in the NIR region of the electromagnetic spectrum. [1,2] NIR polymethine dyes, such as pentamethine and heptamethine cyanines and squaraines, are well suited for this purpose and have been extensively studied for these applications.[3–7] The same strengths that have promoted their development as NIR probes, make these dyes potential candidates as photosensitizers in photodynamic therapy (PDT).[8–11] PDT is a minimally invasive approach exploiting the biological consequences of localized oxidative damage generated by photodynamic processes.[12] Every initial photodynamic process is characterized by the presence of a light-activated drug called photosensitizer (PS), light and oxygen. The PS is excited by a non-thermal light (i.e. LED) at the appropriate excitation wavelength, upon a certain time (drug-to-light interval, DLI) from the administration to the patient. The deactivation of the PS excited state (PS*) occurs mainly by two photochemical processes of relevance in PDT: photoelectric electron transfer or energy transfer from PS* to another molecule like molecular oxygen,

generating reactive oxygen species (ROS) such a singlet oxygen $^1O_2$.[13–15] An appropriate choice of the PS is of great importance to maximize the treatment effectiveness by high ROS production.

Among the proposed PS,[16,17] polymethine and cyanine dyes, show the desired characteristics of PDT-active photosensitizer.[18] In particular, the easiness in designing NIR molecules provides cyanines with absorption in the phototherapeutic window (600-850 nm). Several *in vivo* imaging and PDT studies using heptamethine cyanine and squaraine dyes have been previously reported.[8,19–21] Unsubstituted indolenine- and benzoindolenine-based heptamethinic cyanines have been reported to preferentially accumulate in tumor tissues[3,22]. This interesting observation prompted us to further explore the biological properties of substituted benzoindolenine ring derivatives. In regards to the substituent nature, two to six carbon length side alkyl chains has been reported to optimize the internalization and retention processes in cell.[3,23] The heavy atom effect is usually addressed by insertion, along the molecular scaffold, of bromine atoms which promotes the intersystem conversion in the excited triplet state of the dye increasing the ROS generation. Similar effect was recently described also for squaraine-based PSs.[8,20]

In the present work we investigated the photodynamic potential of a new series of NIR dyes. A new series of NIR symmetrical cyanine dyes, based on a benzoindoleninic ring (Fig. 1), was synthetized and photophysically characterized before being *in vitro* tested for the evaluation of their cytotoxicity and photo-toxicity.

The heteroaromatic benzoindolenine ring of various symmetrical cyanine dyes has been differently substituted and quaternarized to implement a structure-activity study and to determine the substitutions influence on the cellular uptake, ROS production and photodynamic activity.

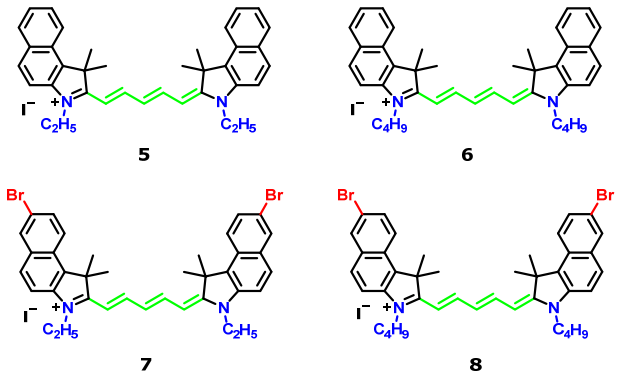

Figure 1. Structures of the synthesized symmetrical cyanine dyes.

2. Experimental details

2.1 Materials and techniques

All the chemicals were purchased from Sigma Aldrich, Fluka, Merck or Riedel de Haen and were used without any further purification.

All microwave reactions were performed in single-mode Biotage Initiator 2.5. TLC were performed on silica gel 60 F254 plates. ESI-MS spectra were recorded using a LCQ Thermo Advantage Max

spectrometer, with electrospray interface and ion trap as mass analyzer. The flow injection effluent was delivered into the ion source using nitrogen as sheath and auxiliary gas. ^{1}H NMR (200 MHz) and ^{13}C NMR (50 MHz) spectra were recorded on a Bruker Avance 200 NMR in $CDCl_3$ or DMSO-d_6.

*2.2. Procedure for the preparation of compounds **1-4***

*2.2.1. (6-bromonaphthalen-2-yl)hydrazine (**1**)*

6-bromonaphthalen-2-ol (21.15 g, 0.95 mol) is cooled down to 0°C in a three-neck flask before hydrazine hydrate (55.18 ml, 1.14 mol) is added drop by drop. The suspension is warmed up to 60-80°C to obtain a clear yellow solution and the reaction is run at 125°C for 24 h. After 24 h, the dark orange reaction mixture is cooled down to 60°C (below this temperature an undesired phase separation takes place). The hot solution is then poured drop by drop in n-propanol. The suspended solid is filtered and washed with n-propanol to provide (6-bromonaphthalen-2-yl)hydrazine (**1**) as a white/yellow solid (3.77 g, 16% yield).

*2.2.2. 7-bromo-1,1,2-trimethyl-1H-benzo[e]indole (**2b**)*

(6-bromonaphthalen-2-yl)hydrazine (**1**) (3.23 g, 13.64 mmol), 3-methylbutan-2-one (4.38 ml, 40.92 mmol) and glacial acetic acid (15 ml) are introduced in a microwave reaction vial, sealed with a crimp cap and heated in the microwave system at 160°C for 10 min. The brown solution is left to cool down and the acetic acid is removed under vacuum. The oily residue is partitioned between diethyl ether (50 ml) and water (150 ml). The aqueous phase is washed three times with petroleum ether (3 x 50 ml). The combined organic solutions are dried and evaporated under vacuum to afford 7-bromo-1,1,2-trimethyl-1H-benzo[e]indole **2b (**3.56 g, yield = 90%) as a brown orange oil.

^{1}H NMR (200MHz, $CDCl_3$), δ: 8.14 (t, J = 4.3 Hz, 1H), 7.85 (dt, J = 14.9, 6.6 Hz, 3H), 7.64 (dd, J = 9.0, 2.0 Hz, 1H), 2.49 (s, 3H), 1.57 (s, 6H).

^{13}C NMR (50MHz, $CDCl_3$), δ: 189.46, 150.56, 138.41, 132.88, 131.03, 129.12, 127.47, 126.56, 123.56, 120.46, 117.70, 76.52, 75.89, 54.81, 22.21.

MS (ESI) $[M+H]^+$ 288.10

*2.2.3. N-((1E,2E)-3-(phenylamino)allylidene)benzenaminium chloride (**3**)*

Compound **3** was prepared as previously described.[24]

^{1}H NMR (200MHz, DMSO-d_6), δ: 12.35 (s, 2H), 8.76 (d, J = 11.3 Hz, 2H), 7.57 – 7.15 (m, 10H), 6.34 (t, J = 11.4 Hz, 1H).

*2.2.4. Synthesis of intermediates (**4a**) and (**4b**)*

The intermediate 3-ethyl-1,1,2-trimethyl-1H-benzo[e]indol-3-ium iodide (**4a**) and 3-butyl-1,1,2-trimethyl-1H-benzo[e]indol-3-ium iodide (**4b**) were prepared as previously described, starting from commercially available **2a**.[25]

*2.2.4.1. Synthesis of 3-ethyl-1,1,2-trimethyl-1H-benzo[e]indol-3-ium iodide (**4a**)*

1H NMR (200 MHz, DMSO) δ 8.50 – 8.02 (m, 8H), 7.90 – 7.60 (m, 4H), 4.61 (q, J = 7.1 Hz, 4H), 2.93 (s, 5H), 1.75 (s, 11H), 1.49 (t, J = 7.2 Hz, 6H).

*2.2.4.2. 3-butyl-1,1,2-trimethyl-1H-benzo[e]indol-3-ium iodide (**4b**)*

MS (ESI) $[M-I]^+$ 266.16

^{1}H NMR (200MHz, DMSO-d6), δ: 8.28 (dt, J = 21.6, 8.6 Hz, 4H), 7.86 – 7.68 (m, 2H), 4.59 (t, J = 7.5 Hz, 2H), 2.91 (d, J = 17.5 Hz, 3H), 2.04 – 1.80 (m, 2H), 1.77 (s, 6H), 1.48 (dd, J = 15.8, 7.3 Hz, 2H), 0.97 (t, J = 6.0 Hz, 3H).

2.3. General quaternization synthesis of bromobenzoindolenine

7-bromo-1,1,2-trimethyl-1H-benzo[e]indole (**2b**), iodoalkane (4 equivalents), and acetonitrile were introduced in a reaction vial, sealed with a crimp cap and heated in microwave system at 155°C for 45 min. The reaction mixture was then poured in diethyl ether (200 ml) to precipitate a brown/green solid which was washed with diethyl ether and filtered.

*2.3.1. 7-bromo-3-ethyl-1,1,2-trimethyl-1H-benzo[e]indol-3-ium iodide (**4c**)*

7-bromo-1,1,2-trimethyl-1H-benzo[e]indole (**2**) (1 g, 3,48 mmol), iodoethane (1,94 ml, 13,9 mmol) and anhydrous acetonitrile (15 ml).

1.19 g, yield = 78%.

^{1}H NMR (200MHz, DMSO-d_6), δ: 8,54 (d, *J* = 2,1 Hz, 1H), 8,29 (dt, *J* = 16,4, 9,0 Hz, 3H), 7,88 (dd, *J* = 9,0, 1,9 Hz, 1H), 4,60 (q, *J* = 7,0 Hz, 2H), 2,89 (s, 3H), 1,74 (s, 6H), 1,49 (t, *J* = 7,3 Hz, 3H).

^{13}C NMR (50MHz, DMSO-d_6), δ: 196.70, 138.93, 134.51, 131.82, 131.52, 130.26, 126.08, 125.95, 120.78, 114.82, 55.78, 43.70, 21.71, 14.00, 13.10.

*2.3.2. 7-bromo-3-butyl-1,1,2-trimethyl-1H-benzo[e]indol-3-ium iodide (**4d**)*

7-bromo-1,1,2-trimethyl-1H-benzo[e]indole (**2**) (1 g, 3,48 mmol), iodobutane (1,58 ml, 13,9 mmol) and anhydrous acetonitrile (15 ml).

1.05 g, yield = 64%.

^{1}H NMR (200MHz, DMSO-d_6), δ: 8,53 (d, *J* = 1,9 Hz, 1H), 8,28 (dt, *J* = 15,4, 9,0 Hz, 3H), 7,87 (dd, *J* = 9,0, 2,0 Hz, 1H), 4,56 (t, *J* = 7,7 Hz, 2H), 2,93 (s, 3H), 1,98 – 1,77 (m, 2H), 1,74 (s, 6H), 1,43 (dt, *J* = 14,7, 7,4 Hz, 2H), 0,94 (t, *J* = 7,3 Hz, 3H).

^{13}C NMR (50MHz, DMSO-d_6), δ: 197.02, 139.22, 137.54, 134.52, 131.83, 131.54, 130.23, 126.04, 125.98, 120.82, 114.98, 55.81, 48.06, 29.71, 21.85, 19.59, 14.19, 13.90.

2.4. General synthesis of symmetrical cyanines

Compounds **4a-d** (2 mol), N-((1E,2E)-3-(phenylamino)allylidene)benzenaminium chloride (**3**) (1 mol), anhydrous sodium acetate (3 mol) and acetic anhydride were introduced in a microwave vial and heated at 130°C for 10-20 min. The reaction mixture was poured in diethyl ether to precipitate a blue solid,

which was washed with diethyl ether and filtered. The blue solid was dissolved in DCM leaving unreacted sodium acetate crystals on the filter funnel. The filtrate was evaporated under vacuum to obtain the cyanine dyes as a blue powder.

2.4.1. ***Dye 5***

3-ethyl-1,1,2-trimethyl-1H-benzo[e]indol-3-ium iodide (**4a**) (500 mg, 1.37 mmol), N-((1E,2E)-3-(phenylamino)allylidene)benzenaminium chloride (**3**) (177 mg, 0.68 mmol), anhydrous sodium acetate (169 mg, 2.05 mmol) and acetic anhydride (15 ml) were introduced in a microwave vial and heated at 130°C for 20 min. **5** as a blue powder (375 mg, yield = 86%).

MS (ESI) $[M-I]^+$ 511.28.

^{1}H NMR (200MHz, DMSO-d_6), δ: 8.46 (t, J = 13.1 Hz, 2H), 8.26 (d, J = 8.3 Hz, 2H), 8.07 (dd, J = 8.2, 5.4 Hz, 4H), 7.70 (dd, J = 16.4, 8.1 Hz, 4H), 7.57 – 7.44 (m, 2H), 6.63 (t, J = 12.2 Hz, 1H), 6.37 (d, J = 13.9 Hz, 2H), 4.28 (d, J = 7.0 Hz, 4H), 1.93 (d, J = 10.8 Hz, 12H), 1.33 (t, J = 7.0 Hz, 6H).

^{13}C NMR (50MHz, DMSO-d_6) δ: 173.48, 153.27, 139.55, 133.50, 131.55, 130.64, 130.21, 128.00, 127.89, 125.78, 125.03, 122.38, 111.66, 102.79, 50.99, 26.95, 12.73.

2.4.2. ***Dye 6***

3-butyl-1,1,2-trimethyl-1H-benzo[e]indol-3-ium iodide (**4b**) (1 g, 2.54 mmol), N-((1E,2E)-3-(phenylamino)allylidene)benzenaminium chloride (**3**) (329 mg, 1.27 mmol), anhydrous sodium acetate (313 mg, 3.81 mmol) and acetic anhydride (15 ml) were introduced in a microwave vial and heated at 130°C for 20 min. **6** as a blue-violet powder (694 mg, yield = 79%).

MS (ESI) $[M-I]^+$ 567.52.

^{1}H NMR (200MHz, DMSO-d_6), δ: 8.47 (t, *J* = 13.1 Hz, 2H), 8.26 (d, *J* = 8.8 Hz, 2H), 8.07 (dd, *J* = 8.2, 4.0 Hz, 4H), 7.71 (dd, *J* = 17.2, 8.1 Hz, 4H), 7.57 – 7.46 (m, 2H), 6.66 (t, *J* = 12.4 Hz, 1H), 6.38 (d, *J* = 13.6 Hz, 2H), 4.24 (t, *J* = 7.5 Hz, 4H), 1.94 (d, *J* = 12.1 Hz, 12H), 1.82 – 1.64 (m, 4H), 1.53 – 1.33 (m, 4H), 0.95 (t, *J* = 7.2 Hz, 6H).

^{13}C NMR (50MHz, DMSO-d_6) δ: 173.89, 153.09, 139.98, 133.40, 131.53, 130.57, 130.19, 128.01, 127.85, 125.05, 122.42, 111.90, 103.24, 50.96, 43.60, 29.66, 27.06, 19.73, 14.06.

2.4.3. ***Dye 7***

7-bromo-3-ethyl-1,1,2-trimethyl-1H-benzo[e]indol-3-ium iodide (**4c**) (500 mg, 1.13 mmol), N-((1E,2E)-3-(phenylamino)allylidene)benzenaminium chloride (**3**) (146 mg, 0.56 mmol), anhydrous sodium acetate (139 mg, 1.69 mmol) and acetic anhydride (15 ml) were introduced in a microwave vial and heated at 130°C for 10 min. **7** as a blue powder (353 mg, yield = 79%).

MS (ESI) $[M-I]^+$ 669.21

^{1}H NMR (200MHz DMSO-d_6), δ: 8.55 – 8.34 (m, 4H), 8.22 (d, *J* = 9.1 Hz, 2H), 8.09 (d, *J* = 9.0 Hz, 2H), 7.77 (dd, *J* = 14.1, 5.3 Hz, 4H), 6.64 (t, *J* = 12.4 Hz, 1H), 6.38 (d, *J* = 14.0 Hz, 2H), 4.28 (t, *J* = 6.8 Hz, 4H), 1.92 (s, 12H), 1.32 (t, *J* = 6.8 Hz, 6H).

^{13}C NMR (50MHz, DMSO-d_6) δ: 172.75, 152.82, 139.45, 133.12, 132.12, 131.25, 130.16, 129.32, 125.69 (d, J = 6.5 Hz), 124.03, 117.18, 112.30, 102.50, 50.30, 26.30, 12.06.

2.4.4. ***Dye 8***

7-bromo-3-butyl-1,1,2-trimethyl-1H-benzo[e]indol-3-ium iodide (**4d**) (500 mg, 1.06 mmol), N-((1E,2E)-3-(phenylamino)allylidene)benzenaminium chloride (**3**) (137 mg, 0.53 mmol), anhydrous sodium acetate (130 mg, 1.59 mmol) and acetic anhydride (15 ml) were introduced in a microwave vial and heated at 130°C for 10 min. **8** as a blue powder (369 mg, yield = 82%).

MS (ESI) $[M-I]^+$ 725.25

^{1}H NMR (200MHz, DMSO-d_6), δ: 8.56 – 8.32 (m, 4H), 8.23 (d, *J* = 9.1 Hz, 2H), 8.08 (d, *J* = 8.9 Hz, 2H), 7.78 (dd, *J* = 14.4, 5.5 Hz, 4H), 6.67 (t, *J* = 12.4 Hz, 1H), 6.39 (d, *J* = 13.8 Hz, 2H), 4.23 (t, 4H), 1.72 (s, 4H), 1.42 (dd, *J* = 15.3, 7.5 Hz, 4H), 0.94 (t, *J* = 7.3 Hz, 6H).

^{13}C NMR (50MHz, DMSO-d_6) δ: 173.99, 153.47, 140.66, 133.85, 132.91, 132.05, 130.99, 130.08, 126.53, 124.87, 118.04, 113.32, 103.73, 51.10, 43.92, 27.25, 19.91, 14.25.

2.5. Spectroscopic characterization of the symmetrical cyanines

2.5.1. UV-Vis spectroscopy

UV-Vis spectra were recorded on a Shimadzu UV-1700 Pharma Spec using different solvents in order to investigate the solvatochromic behavior of the symmetrical cyanines. A stock solution (0.7 mM) in absolute ethanol (EtOH) was prepared and diluted solutions in acetone, dimethylformamide (DMF), methanol, acetonitrile, tetrahydrofuran (THF), dichloromethane (DCM) and DMSO were analyzed.

2.5.1.1. Determination of Molar Extinction Coefficient

A concentrated solution per each dye was prepared by weighting the dyes (5-7 mg) and dissolving them in 10 ml of absolute ethanol (EtOH). Three diluted solution (25 ml) of EtOH were prepared by taking aliquots (0.2, 0.1 and 0.05 ml) of the stock solution. The diluted solutions were measured by UV-Vis spectroscopy (Shimadzu UV-1700) using quartz cuvettes (1 cm pathway length). The absorbance intensities of each solution at the λ_{max} were plotted versus the sample concentration. A linear fit was applied to determine the molar extinction coefficient (ε) as the slope of the line. The analysis was performed in duplicate. The obtained data were considered acceptable when the difference between the determined log ε was less or equal to 0.02 in respect to their average. Otherwise new concentrated dye stock solution in absolute EtOH was prepared and the protocol repeated.

2.5.2. Fluorescence spectroscopy

Fluorescence measurements were recorded using a HORIBA Jobin Yvon Fluorolog 2. Diluted solutions with absorbance around or lower of 0.1 units were used to avoid the presence of aggregates. Fluorescence lifetimes were obtained using a proper NanoLED source (636 nm) and a photon counting detector (TBX04). The data were fitted to a single exponential function giving the lifetime. The

goodness of the fit was assessed by the chi-squared value of less than 1.05 and a residual trace that was symmetric about the zero axes. Fluorescence quantum yields were determined using the same instrument with Quanta-φ integrating sphere and De Mello method. The final result is an average of three independent measurements.

2.6. Biological assays

2.6.1. Cell line and cytotoxicity assay

The human fibrosarcoma cell line, HT-1080, was obtained from the American Type Culture Collection (ATCC, Rockville, MD, USA). HT-1080 cells were grown as a monolayer culture in Eagle's Minimum Essential Medium (EMEM, Sigma-Aldrich, Milano, Italy) supplemented with 10% heat-inactivated fetal calf serum, 2 mM L-glutamine, 100 UI/mL penicillin and 100 µg/mL streptomycin (Sigma-Aldrich), at +37°C in a humidified atmosphere of 5% CO_2 in air. HT-1080 cells in the exponential growth phase were detached using 0.05% trypsin-0.02% EDTA solution (Sigma-Aldrich), resuspended in culture medium and seeded at the appropriate cell concentration for cell culture experiments.

The WST-1 cell proliferation assay was used to evaluate the cytotoxic effect on HT-1080 cells of cyanine dyes, *i.e.*, **5**, **7**, **6** and **8**, to select the concentration suitable for the *in vitro* PDT. Specifically, $1.5x10^3$ cells were seeded in 100 µL of culture medium in replicates (n = 8) in 96-well culture plates (TPP, Trasadingen, Switzerland), and after 24 h of cell growth the medium was removed, and the cells incubated with experimental media of differing cyanine dyes' concentrations (1, 10, 50 and 100 nM). The WST-1 reagent (Sigma-Aldrich, 10 µL/100 µL) was added at 24, 48, and 72 h and the plates were incubated at +37°C in 5% CO_2 in air for 1.5 h. The well absorbance was measured at 450 and 620 nm (reference wavelength) in a microplate reader (Asys UV340; Biochrom, Cambridge, UK).

2.6.2. Flow cytometric analysis

The cellular uptake of cyanine dyes, *i.e.*, **5**, **6, 7** and **8**, was evaluated by a flow cytometric analysis (BD Accuri C6, Becton, Dickinson Bioscience, Milano, Italy). Briefly, 1.5×10^5 cells were plated in 6-well culture plates (TPP) and after 24 h incubated with cyanine dyes at the maximum non-cytotoxic concentration tested (10 nM) for 1, 4 and 24 h. Cells were then detached after each incubation period using a 0.05% trypsin-0.02% EDTA solution (Sigma Aldrich) and re-suspended in 300 µL of phosphate buffered solution (PBS, Sigma Aldrich). Cells were then run on the flow cytometer considering 10,000 events at a 640 nm excitation to measure the intracellular dye.

Reactive oxygen species (ROS) production was evaluated 1, 5, 15, 30, 45, 60 min after the *in vitro* PDT with the different cyanine dyes carried out as described below. HT-1080 cells were incubated with 10 µM of 2',7'-dichlorofluorescein diacetate (DCFH-DA) (Sigma Aldrich) for 30 min, 1 h after incubation with cyanine dyes, *i.e.*, **5**, **6, 7** and **8** at 10 nM. After the *in vitro* PDT, cells were analyzed for ROS production by flow cytometry evaluating 10,000 events at a 488 nm excitation. ROS production was

expressed as integrated median fluorescence intensity (iMFI), which is the product of the frequency of ROS-producing cells and the median fluorescence intensity of the cells.

2.6.3. In vitro photodynamic treatment

HT-1080 cells in the exponential phase were pre-incubated in the dark for 1 h, the time needed for an efficient internalization, in a culture medium containing cyanine dyes at 10 nM, *i.e.*, the maximum non-cytotoxic concentration tested. Cells were removed from the flask after incubation using a 0.05% trypsin-0.02% EDTA solution (Sigma Aldrich) and normalized to 1.5 x 10^5 cells in 1 mL of PBS in polystyrene tubes (TPP). The light-emitting source was based on a light beam (LB), specifically a red LED with a wavelength of 636 nm and energy fluency rates adjusted to 15 mW/cm^2. Briefly, cellular suspensions were exposed to the LB for 20 min in a dark box. After PDT, 1.5 x 10^3 cells were plated in a 96-well culture plate (TPP) and cell proliferation was evaluated at 24, 48 and 72 h using the WST-1 cell proliferation reagent (10 µL/100 µL). Cell proliferation data are expressed as a percentage of the absorbance of treated cells *vs* untreated cells.

2.6.4. Statistical analysis

Data are shown as average values of three independent experiments ± standard deviation. Statistical analyses were performed using Graph-Pad Prism 5.0 software (La Jolla, CA, USA); one-way and two-way analyses of variance and Bonferroni's test were used to calculate the threshold of significance. Statistical significance was set at $p < 0.05$.

3. Results and discussion

3.1. Synthesis

The synthesis of symmetrical brominated and non-brominated pentamethine cyanine dyes involved the condensation of the quaternary heterocyclic salts, bearing an activated methyl group, with malonodialdehyde derivatives.[24] While 1,1,2-trimethyl-1H-benzo[e]indole (**2a**) is commercially available, the 7-bromo-1,1,2-trimethyl-1H-benzo[e]indole (**2b**) was readily obtained exploiting the Fischer indole synthesis by reacting (6-bromonaphthalen-2-yl)hydrazine with 3-methylbutan-2-one in glacial acetic acid, as previously described for the reported bromoindolium iodide[26] and carboxybenzoindolium iodide[27] (see Scheme 1). The subsequent quaternization of the benzoindolenine ring, performed under microwave irradiation[26,27], led to an increased acidity of the methyl group which enabled the cyanine bridge formation (see first step in Scheme 2).

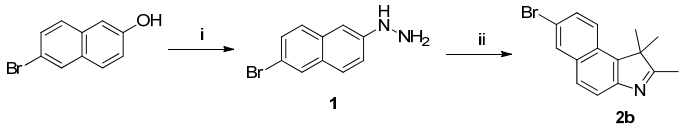

Scheme 1. Synthesis of bromobenzoindolenine. Experimental conditions: (i) hydrazine hydrate, 0°C; 125°C, 24 h; (ii) 3-methylbutan-2-one, glacial acetic acid, MW, 10 min, 160°C.

The characterization of quaternarized salts of 1,1,2-trimethyl-1H-benzo[e]indole (**4a-b**) matched the previously reported in literature.[25] All the symmetrical cyanine dyes were synthesized in a one-step reaction under microwave heating following a green method published by Owens et al.[28] by reacting two equivalents of quaternary heterocyclic salts with the malonoaldehyde bis(phenylimine)monohydrochloride (**3**) in the presence of sodium acetate and acetic anhydride (see Scheme 2). The reaction mixture was finally poured in diethyl ether to precipitate a blue solid, which was washed and filtered. Unreacted sodium acetate crystals were then removed by DCM. Finally, cyanine dyes were obtained in good yields (79-86%).

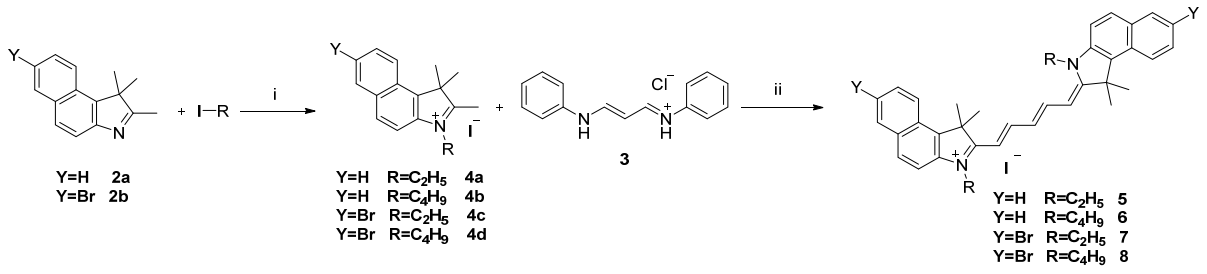

Scheme 2. Synthesis of **5**, **6**, **7** and **8** dyes. Experimental conditions: (i) anhydrous acetonitrile, iodoalkane, MW, 45 min, 155°C; (ii) sodium acetate, acetic anhydride, MW, 10/20 min, 130°C.

3.2. Spectroscopic characterization of the symmetrical cyanine dyes

All compounds show a narrow absorption band in the NIR, perfectly matching the phototherapeutic window, with the hypsochromic shoulder typical for cyanine dyes. The electronic absorption and emission spectra of the compounds, in EtOH, are depicted in Figure 2 while the main photophysical parameters in EtOH and DMSO are reported in Table 1 and 2. Different substituents (i.e., presence or absence of Br and length of the alkyl chain) on the benzoindolenine ring have no effect on the λ_{max} suggesting that the electronic levels, involved in the π-π* transition, have similar energies.[29] All the compounds are characterized by an absorption maximum around 680-695 nm and molar extinction coefficient varying from 160,000 to 225,000 $M^{-1}cm^{-1}$.

The solvatochromic effect on the compounds absorption spectra was also investigated as depicted in Figure 3 for dye **5**. As general trend, neither the absorption maxima nor the band shape are affected by the solvent polarity. DCM induces a 15 nm bathochromic shift in comparison to MeOH suggesting a more polar ground state in comparison to the excited one. No significant differences were observed in the absorption peak maxima in protic or aprotic solvents. Similar effect was recorded in the emission spectra. Moreover, the low Stokes shift (20 nm) value indicates that a moderate geometry change occurs from the ground to the excited state.

Fluorescence lifetimes (τ_f) show monoexponential decay and are in the ns range. The alkyl chain length on the benzoindolenine ring slightly influences τ_f. A small τ_f increase is evident with longer chains, both on brominated and non-brominated dyes. The fluorescence quantum yield shows an opposite behaviour varying from 29 to 38% as expected for cyanine dyes.

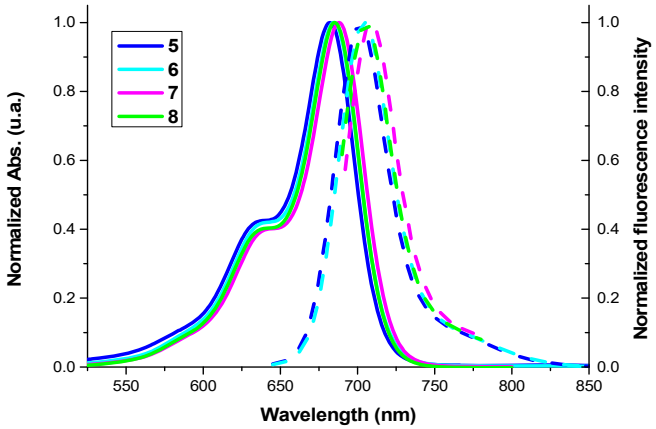

Figure 2. Normalized UV-Vis and fluorescence spectra of the synthesized symmetrical cyanine dyes in absolute ethanol.

Table 1

Selected photophysical properties of symmetrical cyanine dyes in absolute ethanol.

Dye	λ_{abs} (nm)	ε ($M^{-1}cm^{-1}$)	λ_{em} (nm)	Stokes shift (nm)
5	682	$1.60 \cdot 10^5$	702	20
6	684	$1.88 \cdot 10^5$	704	20
7	685	$2.25 \cdot 10^5$	705	20
8	688	$2.08 \cdot 10^5$	709	21

Table 2

Fluorescence lifetime and quantum yields of symmetrical cyanine dyes in DMSO.

Dye	λ_{abs} (nm)	λ_{em} (nm)	Stokes shift (nm)	Φ (%)	τ_f (ns)
5	686	705	19	30.2	1.31
6	689	709	20	29.1	1.42
7	689	709	20	38.1	1.45
8	692	713	19	36.5	1.57

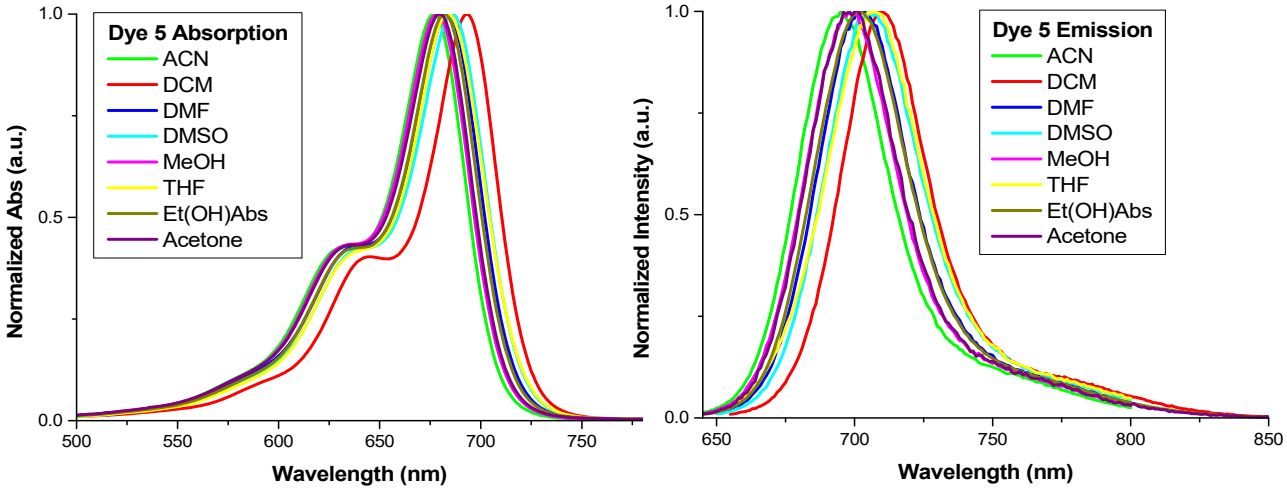

Figure 3. Solvatochromic behavior of dye **5**.

3.3. In vitro photodynamic activity

3.3.1. Effect of cyanine dye-based photodynamic treatment on HT-1080 cell proliferation

HT-1080 cells were exposed to increasing concentration (1, 10, 50 and 100 nM) of each cyanine dye, *i.e.*, **5**, **6, 7** and **8**, to determine the maximum non-cytotoxic concentration suitable for performing the *in vitro* PDT. A dose-dependent cytotoxicity was observed for all the cyanine dyes (Figure 4). All the

cyanine dyes induced a decrease of HT-1080 cell proliferation after 48 h of incubation at the highest concentration of 100 nM (**5** $p < 0.01$; **7**, **6** and **8** $p < 0.001$), while at 50 nM the decrease of cell proliferation was of course more modest (**5** $p < 0.01$; **7** and **6** $p < 0.001$). Interestingly, **6** was the only dye that induced a significant cytotoxicity already after 24 h of incubation either at 50 nM ($p < 0.01$) and 100 nM ($p < 0.001$). On the other hand, the brominated derivative **8** almost unaffected HT-1080 cell proliferation until 72 h of incubation at 50 nM and produced a lower decrease of cell proliferation at 100 nM when compared to the other cyanines. Based on these results, the highest non-cytotoxic concentration was 10 nM for all the examined cyanine dyes (Figure 4).

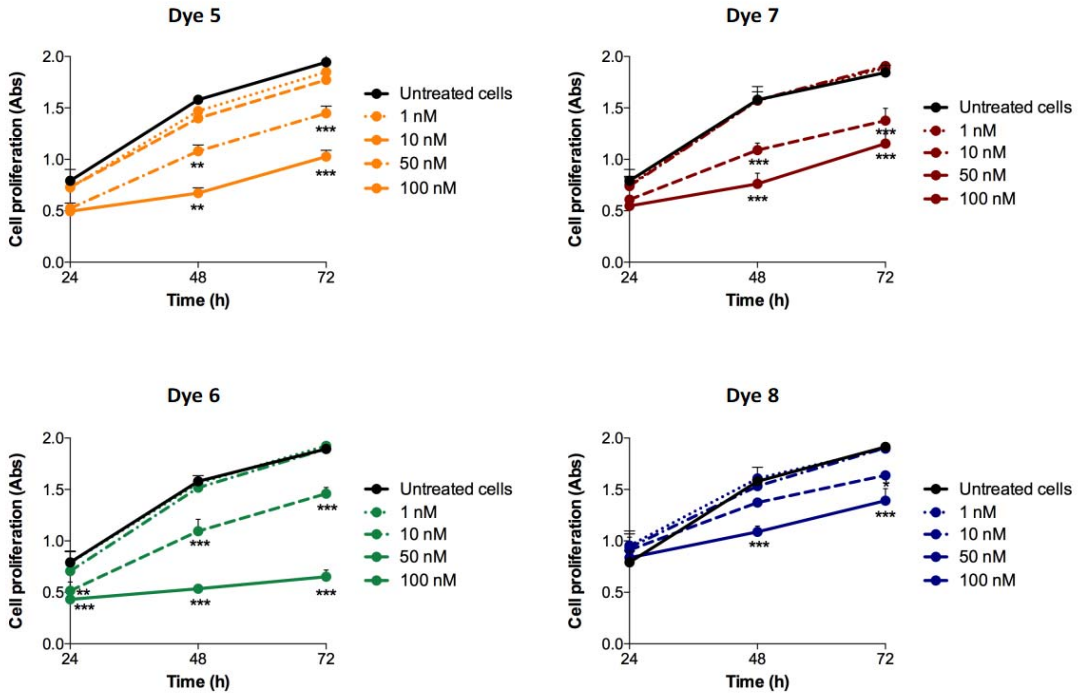

Figure 4. Effects of cyanine dyes on HT-1080 cell proliferation. Cell proliferation, after exposure to increasing concentrations of cyanine dyes (1, 10, 50, 100 nM), was evaluated at 24, 48 and 72 h by WST-1 assay. Statistical significance *vs* untreated cells: $^{**}p < 0.05$, $^{**}p < 0.01$, $^{***}p < 0.001$.

The HT-1080 cell uptake of cyanine dyes was then evaluated cytofluorimetrically after 1, 4 and 24 h of incubation of the cells with the minimum non-cytotoxic concentration *i.e.* 10 nM. All the cyanine dyes were efficiently internalized by HT-1080 cells just after 1 h of incubation (Figure 5), suggesting a rapid and effective cellular uptake which could be related to the lipophilic/cationic structure of these dyes.

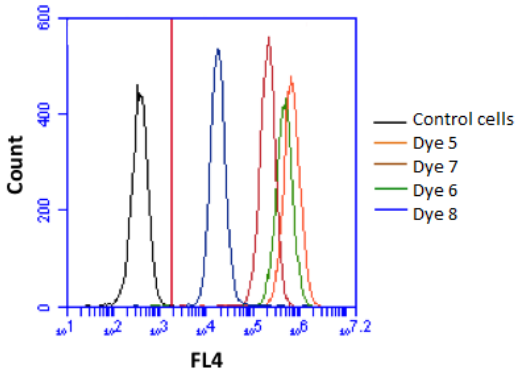

Figure 5. Flow cytometric analysis of cyanine dyes' cell uptake. HT-1080 cells were incubated with cyanine dyes at the same concentration (10 nM) for 1 h. Fluorescent signal was detected using a flow cytometer at 640 nm excitation (FL4) to measure the cellular cyanine dye fluorescence with respect to untreated cells (control cells).

Once obtained the minimum non-cytotoxic concentration and the specific time for cyanine dyes uptake, the potential photocytotoxicity of each cyanine dye was evaluated by performing an *in vitro* photodynamic treatment.

The light-induced cytotoxic effect of each cynine dye was observed up to 72 h after the photodynamic treatment. While HT-1080 cell proliferation was unaffected by control treatments, i.e., exposure to cyanine dye (10 nM) or light beam alone (LB, 15 mW/cm^2 for 20 min), a cytotoxic photodynamic effect was observed with each cyanine dye, becoming more significant at 72 h after PDT. In comparison to untreated HT-1080 cells, a slight cell proliferation reduction was observed for **5** (70.9% ± 18.3%, $p < 0.05$) while stronger reduction was reported with **7** (53.6% ± 13.3%, $p < 0.001$), **6** (49.1% ± 10.2%, $p < 0.001$) and **8** (56.7% ± 10.5%, $p < 0.001$) 72 h after PDT. Surprisingly, a very small difference in the photoactivity behavior was found when comparing **6** with the brominated analog **8**. The heavy atom effect on the PDT activity is well-known documented for similar series of indolenine based cyanine[19] and squaraine dyes.[20] This different behaviour could be explained by the relative position of the bromine on the dye structure. The heavy atom effect is remarkable when directly linked to an indolenine ring. In the present work the bromine atom is on a benzoindolenine structure. We speculate that this position could have certain effect on the distance and on the effect on the dye photoactivity. On the other hand, the longer alkyl chains connected to the cyanine structure favour the photoactivity as reported in literature.[23]

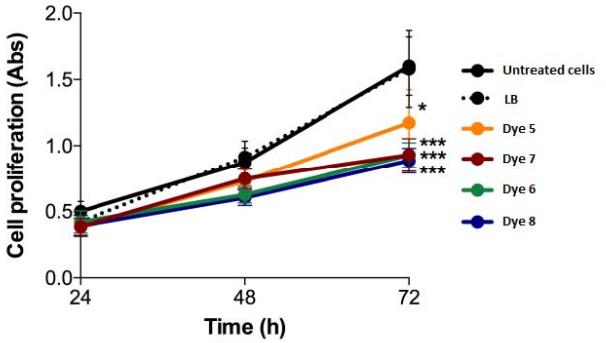

Figure 6. Effect of photodynamic treatment on HT-1080 cell proliferation. Cells were incubated for 1 h with different cyanine dyes at the same concentration (10 nM) and then exposed to PDT with a light beam (LB, 636 nm) at 15 mW/cm^2 for 20 min. Cell proliferation was evaluated after 24, 48 and 72 h by WST-1 assay. Statistically significant difference *vs* untreated cells: *$p < 0.05$, ***$p < 0.001$.

3.3.2. Effects of cyanine dye-based photodynamic treatment on reactive oxygen species production

DCFH-DA (2',7'-dichlorofluorescin diacetate) was used as ROS probe to evaluate the intracellular ROS generation after PDT by flow cytometry. Highly fluorescent DCF is generated in presence of peroxides and can be excited at 488 nm where the synthetized cyanine dyes do not absorb light. **5** showed a different ROS generation pattern with respect to other cyanine dyes, maybe in line with its different photodynamic cytotoxic effect. An increased intracellular production of ROS, reaching a maximum 45 minutes after the photodynamic treatment was observed upon irradiation at proper wavelength of **5**. On the other hand, **7**, **6** and **8** showed a rapid increase in ROS production after the photodynamic treatment with a reaching the highest ROS value after 1, 15 and 1 min, respectively. Similar ROS production decrease that reset after 45 min from the photodynamic treatment was observed for **7** and **8**.

It is worth noting that the cyanine dyes which produce higher values of ROS in the shorter time in *i.e.*, **7**, **8** and **6**, are the more photo-cytotoxic in the *in vitro* PDT treatment (Figure 6). Finally, it has to be pointed out that the highest ROS production values were obtained by treatment with **5** and **7** 45 and 1 minute after light exposure respectively.

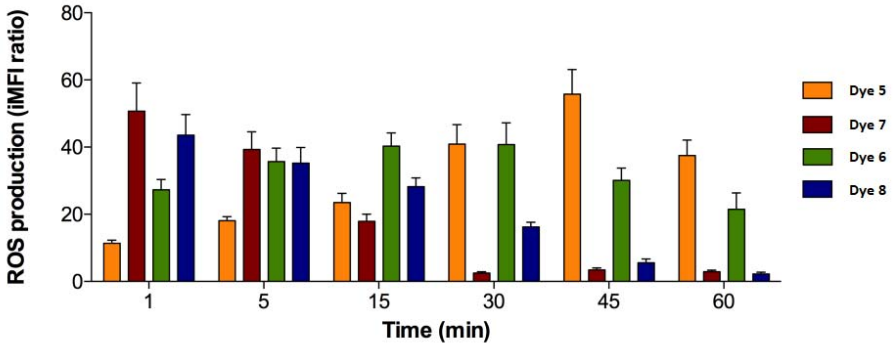

Figure 7. HT-1080 reactive oxygen species (ROS) production after PDT. HT-1080 cells were exposed to PDT with a light beam (LB, 636 nm) at 15 mW/cm^2 for 20 min, alone or after cell incubation for 1 h with cyanine dyes at the same concentration (10 nM). ROS levels were determined according to the dichlorofluorescin-diacetate assay by flow cytometry and expressed as the integrated median fluorescence ratio (iMFI), as described in Materials and Methods.

4. Conclusions

We have reported the synthesis of new symmetrical brominated and non-brominated penthametine cyanine dyes varying the alkyl chain lengths which confer different lipophilicity characteristics. The absorption maxima around 680-695 nm are not affected by the different substituent on the benzoindolenine ring (i.e. length of the alkyl chain). We have demonstrated that, different from other reported photosensitizers, the presence of a heavy atom such bromine has no remarkable influence on the photodynamic effect for this series of probes. All the tested cyanine dyes show a certain phototoxicity which is slightly higher for the brominated-cyanine with longer alkyl chain (four carbons). Moreover, both brominated and non-brominated benzoindolenine-based cyanines were able to produce ROS and were efficiently internalized by HT-1080 cells just after 1 h of incubation. To our surprise, the presence of bromine on the benzoindolenine ring was depicted by a faster rate of ROS production but has no effect on the photoactivity experiments. This behavior can be explained by the different position of the heavy atom with respect to the other series of polymethine dyes reported in literature. It is worth noting that these molecules are active at very low concentration (10 nM), making them suitable and appealing for *in vivo* application with the possibility of low dose effectiveness.

Acknowledgements

Authors acknowledge the financial support from the University of Torino (Ricerca Locale ex-60%, Bando 2016).

References

[1] Luo S, Zhang E, Su Y, Cheng T, Shi C. A review of NIR dyes in cancer targeting and imaging.

Biomaterials 2011;32:7127–38. doi:10.1016/j.biomaterials.2011.06.024.

[2] Fabian J, Nakazumi H, Matsuoka M. Near-Infrared Absorbing Dyes. Chem Rev 1992;92:1197–226. doi:10.1021/cr00014a003.

[3] Zhang C, Liu T, Su Y, Luo S, Zhu Y, Tan X, et al. A near-infrared fluorescent heptamethine indocyanine dye with preferential tumor accumulation for in vivo imaging. Biomaterials 2010;31:6612–7. doi:10.1016/j.biomaterials.2010.05.007.

[4] Pauli J, Vag T, Haag R, Spieles M, Wenzel M, Kaiser WA, et al. An in vitro characterization study of new near infrared dyes for molecular imaging. Eur J Med Chem 2009;44:3496–503. doi:10.1016/j.ejmech.2009.01.019.

[5] Shimi M, Sankar V, Rahim MKA, Nitha PR, Das S, Radhakrishnan K V., et al. Novel glycoconjugated squaraine dyes for selective optical imaging of cancer cells. Chem Commun 2017;53:1–4. doi:10.1039/c6cc10282d.

[6] Bertolino CA, Caputo G, Barolo C, Viscardi G, Coluccia S. Novel heptamethine cyanine dyes with large stoke's shift for biological applications in the near infrared. J Fluoresc 2006;16:221–5. doi:10.1007/s10895-006-0094-8.

[7] Miletto I, Gilardino A, Zamburlin P, Dalmazzo S, Lovisolo D, Caputo G, et al. Highly bright and photostable cyanine dye-doped silica nanoparticles for optical imaging: Photophysical characterization and cell tests. Dye Pigment 2010;84:121–7. doi:10.1016/j.dyepig.2009.07.004.

[8] Avirah RR, Jayaram DT, Adarsh N, Ramaiah D. Squaraine dyes in PDT: from basic design to in vivo demonstration. Org Biomol Chem 2012;10:911. doi:10.1039/c1ob06588b.

[9] Shi C, Wu JB, Pan D. Review on near-infrared heptamethine cyanine dyes as theranostic agents for tumor imaging, targeting, and photodynamic therapy. J Biomed Opt 2016;21:50901. doi:10.1117/1.JBO.21.5.050901.

[10] Barbero N, Visentin S, Viscardi G. The different kinetic behavior of two potential photosensitizers for PDT. J Photochem Photobiol A Chem 2015;299:38–43. doi:10.1016/j.jphotochem.2014.11.002.

[11] Miletto I, Fraccarollo A, Barbero N, Barolo C, Cossi M, Marchese L, et al. Mesoporous silica nanoparticles incorporating squaraine-based photosensitizers: a combined experimental and computational approach. Dalt Trans 2017:15–8. doi:10.1039/C7DT03735J.

[12] Rkein AM, Ozog DM. Photodynamic therapy. Dermatol Clin 2014;32:415–25.

doi:10.1016/j.det.2014.03.009.

[13] Plaetzer K, Krammer B, Berlanda J, Berr F, Kiesslich T. Photophysics and photochemistry of photodynamic therapy: Fundamental aspects. Lasers Med Sci 2009;24:259–68. doi:10.1007/s10103-008-0539-1.

[14] Macdonald I, Dougherty T. Basic principles of photodynamic therapy. J Porphyrins 2001:105–29.

[15] Ogilby PR. Singlet oxygen: there is indeed something new under the sun. Chem Soc Rev 2010;39:3181. doi:10.1039/b926014p.

[16] Ormond AB, Freeman HS. Dye sensitizers for photodynamic therapy. Materials (Basel) 2013;6:817–40. doi:10.3390/ma6030817.

[17] Baldassarre F, Foglietta F, Vergaro V, Barbero N, Capodilupo AL, Serpe L, et al. Photodynamic activity of thiophene-derived lysosome-specific dyes. J Photochem Photobiol B Biol 2016;158:16–22. doi:10.1016/j.jphotobiol.2016.02.013.

[18] Dichiara M, Prezzavento O, Marrazzo A, Pittalà V, Salerno L, Rescifina A, et al. Recent advances in drug discovery of phototherapeutic non-porphyrinic anticancer agents. Eur J Med Chem 2017. doi:10.1016/j.ejmech.2017.08.070.

[19] Atchison J, Kamila S, Nesbitt H, Logan KA, Nicholas DM, Fowley C, et al. Iodinated cyanine dyes: a new class of sensitisers for use in NIR activated photodynamic therapy (PDT). Chem Commun 2017;53:2009–12. doi:10.1039/C6CC09624G.

[20] Serpe L, Ellena S, Barbero N, Foglietta F, Prandini F, Gallo MP, et al. Squaraines bearing halogenated moieties as anticancer photosensitizers: Synthesis, characterization and biological evaluation. Eur J Med Chem 2016;113:187–97. doi:10.1016/j.ejmech.2016.02.035.

[21] Yang X, Shi C, Tong R, Qian W, Zhau HE, Wang R, et al. Near IR heptamethine cyanine dye-mediated cancer imaging. Clin Cancer Res 2010;16:2833–44. doi:10.1158/1078-0432.CCR-10-0059.

[22] Wang Y, Liu T, Zhang E, Luo S, Tan X, Shi C. Preferential accumulation of the near infrared heptamethine dye IR-780 in the mitochondria of drug-resistant lung cancer cells. Biomaterials 2014;35:4116–24. doi:10.1016/j.biomaterials.2014.01.061.

[23] Onoe S, Temma T, Shimizu Y, Ono M, Saji H. Investigation of cyanine dyes for in vivo optical imaging of altered mitochondrial membrane potential in tumors. Cancer Med 2014;3:775–86. doi:10.1002/cam4.252.

[24] Pisoni DS, Ce A, Borges A, Petzhold CL, Rodembusch FS, Campo LF. Symmetrical and Asymmetrical Cyanine Dyes. Synthesis, Spectral Properties, and BSA Association Study 2014.

[25] Winstead AJ, Nyambura G, Matthews R, Toney D, Oyaghire S. Synthesis of quaternary heterocyclic salts. Molecules 2013;18:14306–19. doi:10.3390/molecules181114306.

[26] Barbero N, Magistris C, Park J, Saccone D, Quagliotto P, Buscaino R, et al. Microwave-assisted synthesis of near-infrared fluorescent indole-based squaraines. Org Lett 2015;17:3306−3309.

[27] Park J, Barbero N, Yoon J, Dell'Orto E, Galliano S, Borrelli R, et al. Panchromatic symmetrical squaraines: a step forward in the molecular engineering of low cost blue-greenish sensitizers for dye-sensitized solar cells. Phys Chem Chem Phys 2014;16:24173–7. doi:10.1039/C4CP04345F.

[28] Owens EA, Bruschi N, Tawney JG, Henary M. A microwave-assisted and environmentally benign approach to the synthesis of near-infrared fluorescent pentamethine cyanine dyes. Dye Pigment 2015;113:27–37. doi:10.1016/j.dyepig.2014.07.035.

[29] Bertolino CA, Ferrari AM, Barolo C, Viscardi G, Caputo G, Coluccia S. Solvent effect on indocyanine dyes: A computational approach. Chem Phys 2006;330:52–9. doi:10.1016/j.chemphys.2006.07.045.